J Therm Anal Calorim (2012) 110:145–152
DOI 10.1007/s10973-011-2186-1

Study of the corrosion products formed on carbon steel surface in hydrochloric acid solution

Adriana Samide · Bogdan Tutunaru · Aurelian Dobritescu · Catalin Negrila

CEEC-TAC1 Conference Special Issue

Abstract Effect of an antibacterial drug, sulfacetamide, IUPAC name *N*-[(4-aminophenyl) sulfonyl] acetamide (APSA), on the corrosion products formed on carbon steel surface in 1.0 mol L^{-1} HCl solution has been investigated using mass loss, X-ray photoelectron spectroscopy (XPS), and simultaneous thermal and differential scanning calorimetry/differential thermal analysis (TG/DSC/DTA). Mass loss measurements reveal that the corrosion rate of carbon steel is retarded by APSA and that the inhibition efficiency of this inhibitor increases with increasing the concentration. XPS analysis shows that, at this stage, the main product of corrosion is a non-stoichiometric Fe^{3+} oxyhydroxide, consisting of a mixture of FeO(OH) in anhydrous or hydrated forms, containing Cl^- inclusions and adsorbed APSA molecules. The mechanism of inhibition was discussed in light of the chemical structure of the investigated inhibitor. The corrosion products were analyzed using TG/DSC/DTA technique.

Keywords Carbon steel · Corrosion inhibition · Mass loss · X-ray photoelectron spectroscopy (XPS) · TG/DSC analysis

A. Samide (✉) · B. Tutunaru · A. Dobritescu
Department of Chemistry, Faculty of Sciences, University of Craiova, 107i Calea Bucureşti, Craiova, Romania
e-mail: samide_adriana@yahoo.com

C. Negrila
National Institute of Materials Physics, 077125 Magurele, Bucharest, Romania

Introduction

Treatments with organic compounds have been proposed in order to improve anticorrosion protection [1–6]. In fact, much attention should be given when selecting inhibitors for investigation or application to ensure the environmental regulations. The inhibitor must be environmentally friendly to replace the older, which is more toxic and harmful to the environment. When applying the ideas of green chemistry to the area of corrosion inhibitors, the major improvement is in the area of eliminating environmentally toxic compounds. Several organic molecules containing sulfur, oxygen, and nitrogen heteroatoms were suggested as inhibitors for steel in acidic medium [7–9]. Many investigators have been reported on the use of antibacterial drugs as corrosion inhibitors [10–16]. Sulfa drugs have been reported also as corrosion inhibitors by several authors [10, 15, 17]. The inhibitive effect of four sulfa drug compounds sulfaguanidine, sulfamethazine, sulfamethoxazole, and sulfadiazine on carbon steel corrosion in HCl solutions was reported using both mass loss and electrochemical measurements such as galvanostatic polarization and EIS [15]. The inhibition mechanism for this class of inhibitors is mainly based on adsorption. The sulfa drugs have a large number of functional adsorption centers (e.g., $–NH_2$ group, $–SO_2–NH–$ group, O and/or *N*-heteroatoms, and aromatic rings). Most of the drugs used play important roles in biological reactions because of their anticonvulsant, antibacterial, antidiabetic, inhibitive to mycobacterium tuberculosis, and other properties [15–17].

The objective of the present study was to investigate the effect of sulfacetamide, IUPAC name *N*-[(4-aminophenyl) sulfonyl] acetamide (APSA), on the corrosion of carbon steel in 1.0 mol L^{-1} HCl solution. The choice of this drug as corrosion inhibitor is based on the following factors: It is

healthy reportedly very important in biological reactions (environmentally friendly); APSA acts as antimicrobial agents by inhibiting bacterial growth; it is easily soluble in water; and its molecules have O and N atoms as active centers.

Experimental

Materials

The experiments were performed with carbon steel, type C38, in the form of plates with the following composition: C = 0.1%, Mn = 0.5%, P = 0.025%, S = 0.025%, and Fe remainder. The aggressive solutions used were made of HCl AR grade. Appropriate concentrations of acid were prepared using distilled water. The following antibacterial drug APSA was used as inhibitor for the corrosion of carbon steel in 1.0 mol L^{-1} HCl. The tested inhibitor was obtained from Fluka, and it is shown in Scheme 1. All the tests were performed in 1.0 mol L^{-1} HCl solution without and with various concentrations of the inhibitor: 4, 6, 8, and 10 mmol L^{-1}.

Mass loss method

Before experiments, the specimens with an area of 4 cm^2 were successively polished with 200, 600, and 800 grade of emery paper, ultrasonically cleaned with bi-distilled water, degreased with acetone, and then stored in a vacuum desiccator. After weighing accurately, the specimens were immersed in 100-mL beaker, which contained 100 mL HCl with and without the addition of different concentrations of inhibitor: 4, 6, 8, and 10 mmol L^{-1}. All the aggressive acid solutions were open to air. Then, the tests were carried out at room temperature (23 ± 1 °C). After 3 days, the specimens were taken out, washed, dried, and weighed accurately. The average mass loss of the carbon steel sheets could be obtained. The corrosion products were obtained by washing some carbon steel plates, followed by drying in an inert atmosphere, at 30 °C.

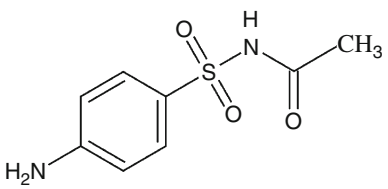

Scheme 1 Chemical molecular structure of *N*-[(4-aminophenyl) sulfonyl] acetamide (APSA)

XPS analysis

X-ray photoelectron spectroscopy (XPS) spectra were recorded in a VG ESCA 3 Mk II-EUROSCAN spectrometer with a Mg K_X-ray source (1486.7 eV photons energy) operated at 300 W (accelerating voltage 12.5 kV, emission current 24 mA). The pressure in the analysis chamber has not exceeded the value of 2–3 × 10^{-8} torr during all the period of spectra acquisition. In order to perform the surface charge compensation, a FG40 flood gun device (Specs Gmbh—Germany) has been used, with a 0.1 mA electronic current at 2 eV energy. The samples have been measured in an "as received" condition with no other surface cleaning treatment (chemical etching or Ar^+ ion beam bombardment). Survey spectra were recorded with a window of 1,200 and 100 eV pass energy. The Gaussian profile lines for curve fitting procedure were used. Binding energy calibration was done by linking the reference to C1*s* line, the binding of C–C or C–H located at 285 eV.

TG/DSC/DTA analysis

In this study, the corrosion products obtained on carbon steel surface in 1.0 mol L^{-1} HCl solution were investigated by TG/DSC/DTA, in nitrogen atmosphere, using a Perkin–Elmer TG/DTA analyzer with Pyris software. The mass of specimen was 2.5 mg. Thermogravimetric measurements were taken in a temperature range of 50–1,000 °C, at a heating rate of 10 °C min^{-1}.

Results and discussion

Mass loss method

The mass loss of carbon steel specimens in 1.0 mol L^{-1} HCl solution, with and without different concentrations from the investigated inhibitor, was determined after 3 days of immersion, at room temperature. From the mass loss measurements, the inhibition efficiency, %IE, of APSA and the corrosion rates, CR, of carbon steel were calculated using Eqs. 1 and 2, respectively:

$$\%\mathrm{IE} = \left(1 - \frac{\mathrm{CR}}{\mathrm{CR}^0}\right) \times 100 \quad (1)$$

$$\mathrm{CR}(\mu m/Y) = \frac{W_t}{A \cdot t \cdot \rho} \times 24 \times 365 \times 10^4 \quad (2)$$

where CR and CR^0 are the corrosion rates (in μm/year) for carbon steel in the presence and absence of the inhibitor in 1.0 mol L^{-1} HCl solution, A is the area of the samples (in cm^2), t is the period of immersion (in hours), W_t is the mass

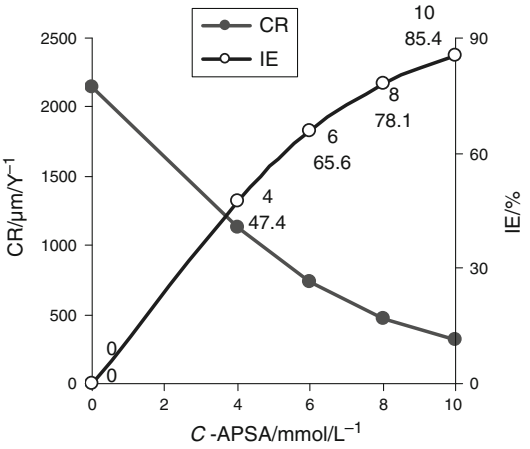

Fig. 1 Corrosion rate and inhibition efficiency of carbon steel corroded in 1.0 mol L^{-1} HCl solution in the absence and the presence of APSA, at room temperature

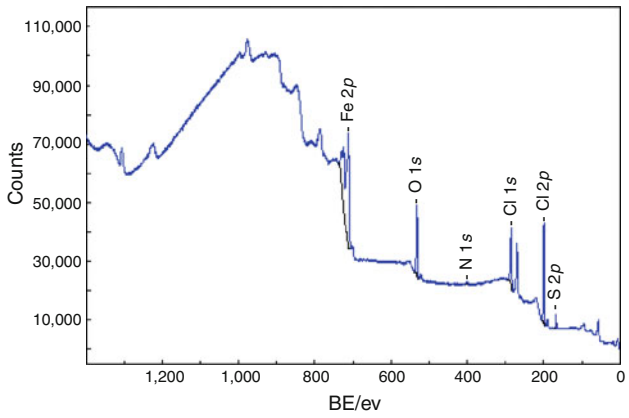

Fig. 2 XPS survey spectrum of carbon steel surface corroded in 1.0 mol L^{-1} HCl solution containing 10 mmol L^{-1} APSA

loss of carbon steel after time t (in g), and ρ is the density of the material (g/cm^3).

Figure 1 shows the variation in mass loss and in inhibition efficiency with concentration of APSA for the corrosion of carbon steel in 1.0 mol L^{-1} solution, at room temperature. It is evident from Fig. 1 that mass loss of carbon steel for the blank solution is higher than that obtained for solutions containing various concentrations of APSA. The plots also indicate that mass loss of carbon steel decreases with increasing concentration of APSA. These also imply that the CR of carbon steel is retarded by APSA and that the inhibition efficiency of inhibitor increases with increasing the concentration reaching a maximum value of 85.4% at 10 mmol L^{-1} APSA in 1.0 mol L^{-1} HCl solution.

XPS analysis

The corroded samples in 1.0 mol L^{-1} HCl solution without and with APSA, after mass loss measurements, were also investigated using XPS surface analysis. The best inhibition occurred when the APSA concentration was 10 mmol L^{-1}.

The XPS survey spectra of carbon steel surface corroded in 1.0 mol L^{-1} HCl blank solution and 1.0 mol L^{-1} HCl solution containing 10 mmol L^{-1} APSA were obtained. Survey spectrum (recorded in a 1,200-eV window) of carbon steel surface corroded in 1.0 mol L^{-1} HCl blank solution shows the peaks at 285, 532, 711, and 199.5 eV binding energy corresponding to C 1*s*, O 1*s*, Fe 2*p*3, and Cl 2*p* lines. Survey spectrum of carbon steel surface corroded in 1.0 mol L^{-1} HCl solution containing 10 mmol L^{-1} APSA shows the peaks at 285, 532, and 711 eV binding energy corresponding to C 1*s*, O 1*s*, and Fe 2*p* lines, and the peaks at 400, 199.5, and 169.0 eV correspond to N 1*s*, Cl 2*p*, and S 2*p* lines, respectively (Fig. 2).

Figure 3 presents the high resolution of XPS spectra for the Fe $2p^{3/2}$, O 1*s*, and Cl 2*p* regions. The binding energies for the peaks have been referenced to C–C bond at 285 eV.

$Fe^{3+}(2p^{3/2})$ appeared at 710.9 and 715.9 eV for the sample which was corroded in 1.0 mol L^{-1} HCl blank solution (Fig. 3a) and at 710.8 and 715.7 eV, respectively, in case the carbon steel was corroded in the presence of APSA (Fig. 3d). The positions and energy are very close to that observed either for FeO(OH) or for Fe_2O_3 structures, respectively [18]. The shake-up of satellites appeared at 715.9 and 715.7 eV, respectively, is also characteristic of Fe^{3+}. From the Fe 2*p* spectra, it can be observed that metallic iron is not detected, because coating thickness is greater than 10–20 atomic layers.

In order to differentiate between FeO(OH) and Fe_2O_3, we also monitored the O 1*s* region (Fig. 3b, e).

The whole set of comparable binding energies obtained for the O 1*s* peak (Fig. 3b, e) deserves some comment. On the high binding energy side, precise assignments are difficult in relation to the existence of ionizations associated with adsorbed species [19]. The analyses have shown: from 529.0 to 531.1 eV, ionization characteristics of oxygen species integrated in the material as O^{2-} and OH^-; from 531.1 to 533 eV, ionization of oxygen species that could allow compensation for some deficiencies in the subsurface of metal oxides. Formally, these oxide ions could be described as O^- species—indeed, owing to a higher covalence of the M–O bonds, these low coordinated oxygen ions would be characterized by a lower electron density than the classical O^{2-} ions [19].

For the oxygen peak of sample corroded in HCl blank solution and in HCl solution containing APSA, three well-resolved peaks were observed at 530.1, 531.8, and 533.1 eV and 530.3, 531.9, and 533.3 eV, respectively, related to metal oxide, hydroxides, and O=S=O/C=O bonds

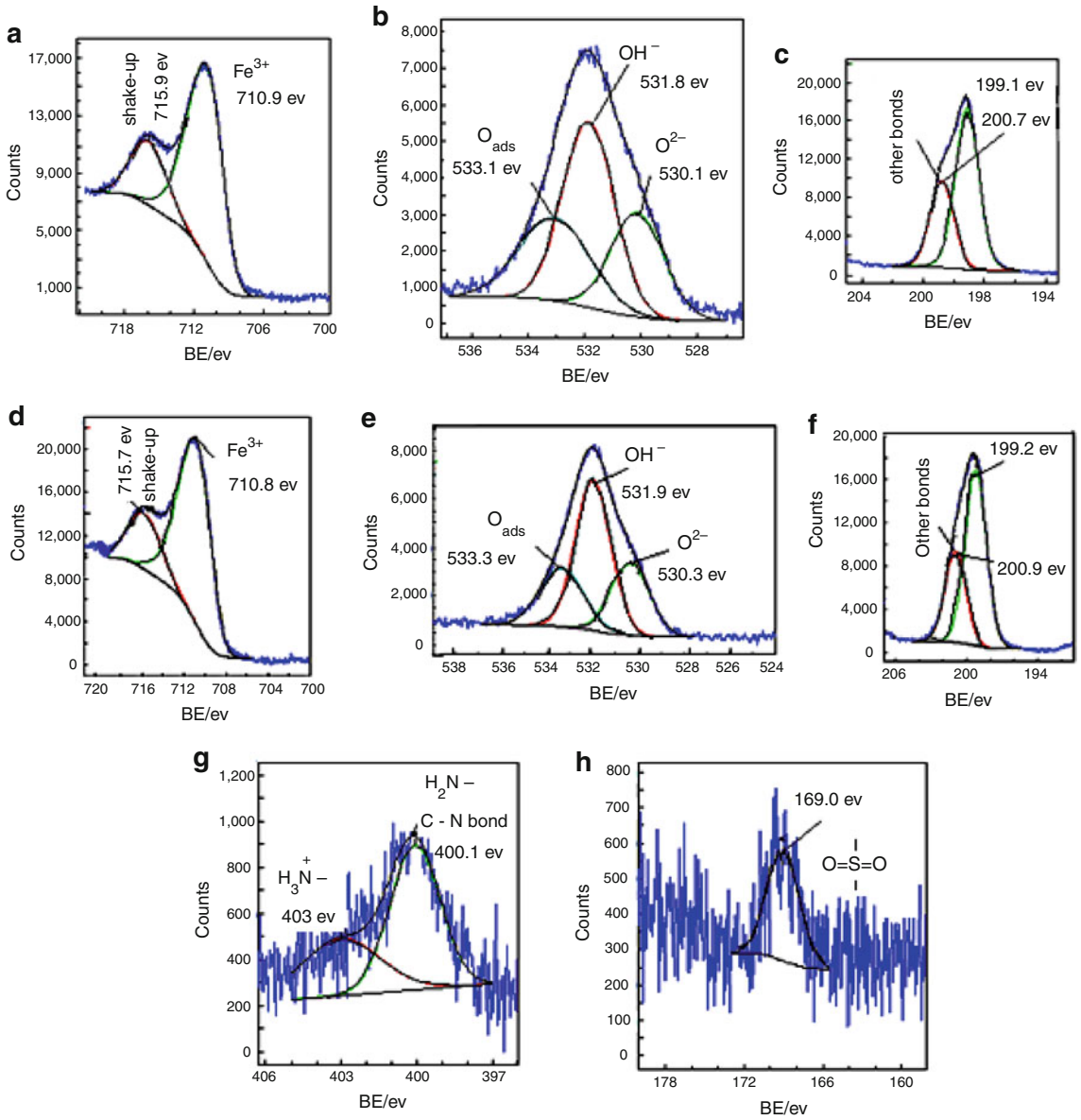

Fig. 3 High resolution of XPS spectra for carbon steel corroded in 1.0 mol L^{-1} HCl blank solution and 1.0 mol L^{-1} HCl solution containing 10 mmol L^{-1} APSA : **a**, **d** Fe 2*p* region; **b**, **e** O 1*s* region; **c**, **f** Cl 2*p* region; **g** N 1*s* spectrum; and **h** S 2*p* spectrum

[20, 21] or other adsorbed species such as oxygen from the water [19]. For FeO(OH), two well-resolved peaks were observed at 530.1/530.3 eV (O^{2-}, Fig. 3b, e) and 531.8/531.9 eV (OH^{-}, Fig. 3b, e). Oxide-hydroxides of iron may occur in anhydrous [FeO(OH)] or hydrated [FeO(OH)·nH_2O] forms, such as ferrihydrite and iron (III) hydroxide [$Fe(OH)_3$].

The Cl 2*p* peak components at the binding energy of about 199.1/200.7 eV (Fig. 3c) and 199.2/200.9 eV (Fig. 3f) are attributable to species such as $Fe^{3+}O$(OH, Cl). No obvious difference is observed between the Cl 2*p* peak of carbon steel surface corroded in 1.0 mol L^{-1} HCl blank solution and carbon steel surface corroded in 1.0 mol L^{-1} HCl solution containing 10 mmol L^{-1} APSA.

The spectral simulation of the N 1*s* photo-peak (Fig. 3g) for carbon steel corroded in the presence of APSA shows organic nitrogen species at 400.1 eV such as amine, amide, imine, etc. [22]. Indeed, this binding energy corresponds to amine group from APSA molecule and/or C–N bonds. Also, at higher energy (403 eV), shoulder is characteristic of the formation of protonated amino group on the carbon steel surface [23].

The S 2*p* level spectrum (Fig. 3h) consists of a peak at high binding energy (169.0 eV). Photo-peak at high binding

energies (169.0 eV) corresponds to highly oxidized (+VI) sulfur such as sulfone [22] from the APSA molecule.

Taking these data into account, we may conclude that, at this stage, the main product of corrosion is a non-stoichiometric Fe^{3+} oxyhydroxide, consisting of a mixture of FeO(OH) and [FeO(OH)·nH_2O], containing Cl^- inclusions and adsorbed APSA molecules.

XPS analysis demonstrated the presence of inhibitor on the steel surface, indicating that the APSA molecules are adsorbed on the substrate and migrated through the concrete layer.

Quantum chemical studies

The researchers are often encouraged to use theoretical data in their studies to support their experimental results. Therefore, recently more corrosion publications contain substantial quantum chemical calculations [24, 25]. GAMEES software package was used in the calculations since it has proved to be highly reliable for calculating the physical properties of molecules. Relationship between molecular structure and their inhibition efficiency was elucidated by ab initio quantum chemical calculations using the density functional theory (DFT). The optimization of initial three-dimensional geometry for APSA molecule was accomplished using B3LYP (Becke 3 Leeyang Parr) hybrid model of density function with electron Gaussian split-valence basis 6–31 ++(*d*, *p*). The optimized HOMO and LUMO structures of investigated inhibitor are given in Fig. 4a–c.

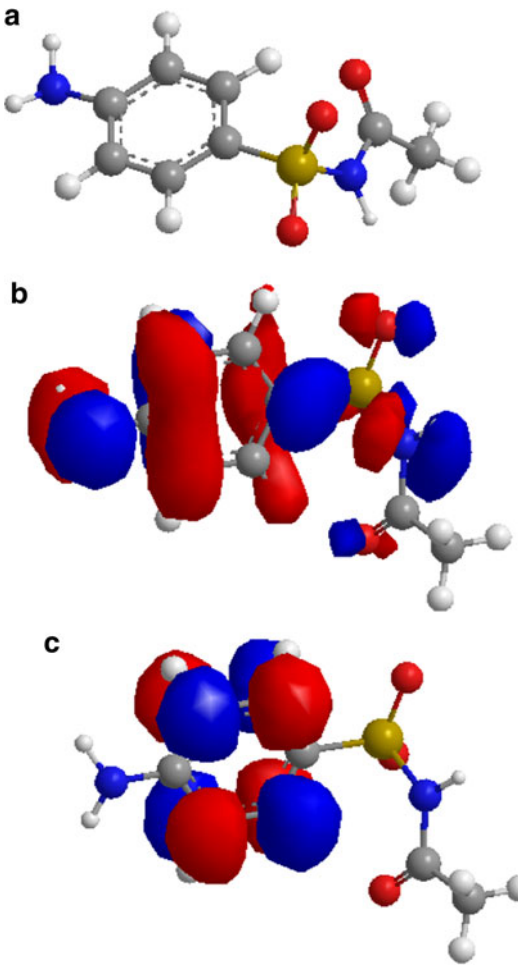

Fig. 4 Optimized (**a**), HOMO (**b**) and LUMO (**c**) structures of investigated inhibitor, *N*-[(4-aminophenyl) sulfonyl] acetamide (APSA)

Several researches have shown that the adsorption of an inhibitor on the metal surface can occur on the basis of donor–acceptor interactions between the *p*-electrons of the investigated compound and the vacant *d*-orbital of the metal surface atoms [26, 27]. Inhibition efficiency, *IE*, of the organic compounds depends on many factors, which include the number of adsorption active centers in the molecule and their charge density, complex formation molecular size, and mode of interaction with metal surface. It is generally believed that the adsorption of the inhibitor at the metal/solution interface is the first step in the mechanism of inhibitor action in aggressive acid media [16].

High E_{HOMO} values indicate that the molecule has a tendency to donate electrons to appropriate acceptor molecules with low-energy empty molecular orbital. The large extension and the obtained value of the APSA E_{HOMO} (−10.909 eV) facilitate adsorption and therefore inhibition, by influencing the transport process through the adsorbed layer. E_{LUMO} values indicate the ability of the molecules to accept electrons. The obtained value of −1.101 eV for APSA E_{LUMO} suggests that the less probable is that sulfacetamide molecule would accept electrons.

The dipole moment ($\mu = 5.51$ D) is another indicator that reflects the electronic density distribution indicating an ionization which facilitates adsorption on carbon steel surface. These results can suggest that the molecules may act as an electron donor when blocking the corrosion reaction. The energy gap ($\Delta E = E_{LUMO} - E_{HOMO} = 9.808$ eV) confirms this mechanism. Moreover, the electron-donating groups enhance adsorption and increase the surface area covered by the compound; also, electron-donating groups with lone pairs on the atoms adjacent to the π system activate the aromatic ring by increasing the electron density on the ring through a resonance donating effect. Also, NH_2-group increases the electron density at the aromatic ring, and it facilitates the adsorption of APSA on the carbon steel.

TG//DSC/DTA results

The resulted rust, as corrosion product of carbon steel in 1.0 mol L^{-1} HCl blank solution and in 1.0 mol L^{-1} HCl containing 10 mmol L^{-1} APSA, was analyzed using TG/DSC/DTA.

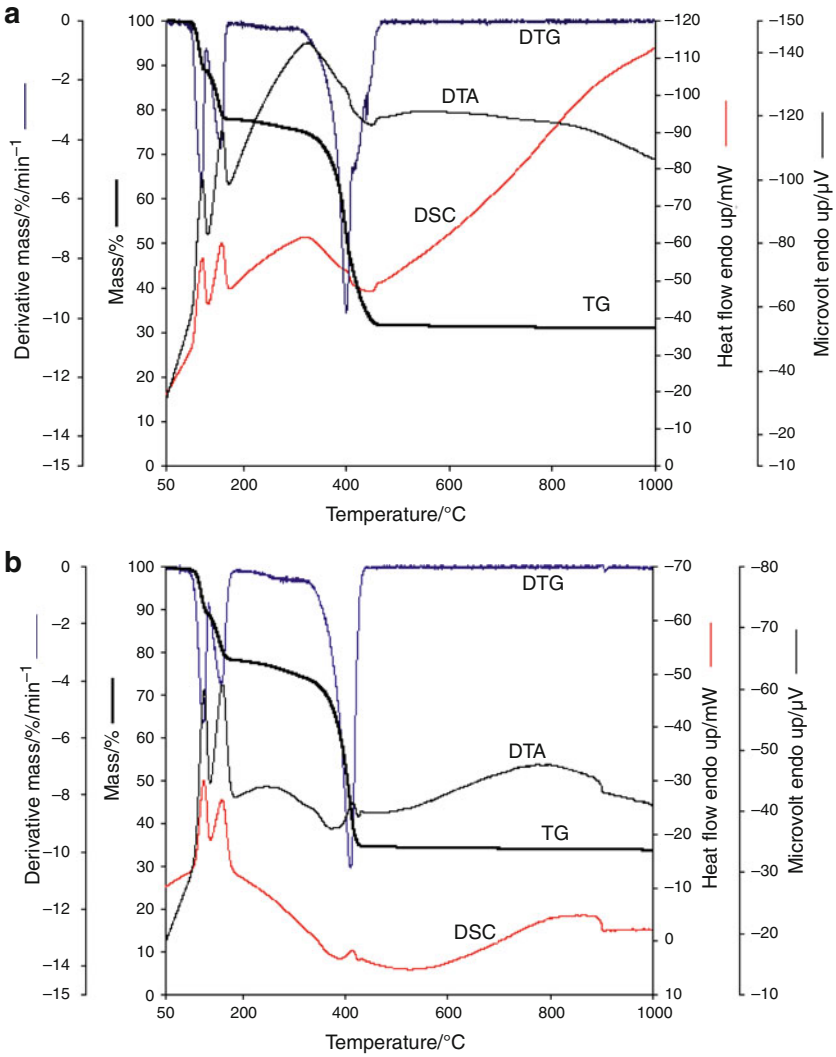

Fig. 5 TG/DTG/DSC/DTA curves for the corrosion product formed in: **a** 1.0 mol L^{-1} HCl blank solution; **b** 1.0 mol L^{-1} HCl solution containing 10 mmol L^{-1} APSA

Table 1 XPS and TG results for the corrosion products formed on carbon steel surface in 1.0 mol L^{-1} HCl solution in the absence and in the presence of APSA, after immersion time of 3 days, at room temperature

Corrosion product	XPS analysis					TG results		
	BE/eV ± 0.1/eV					Process	Temp/°C	Product
	Fe^{3+}	O^{2-}	OH^-	O_{ads}	Cl^-			
C-steel/1.0/mol/L HCl blank solution								
FeO(OH) anhydrous and hydrated	710.9	530.1	531.8	533.1	–	Desorption of physically adsorbed water	50–164.5	Stable corr. product
$Fe^{3+}O(OH, Cl)$	710.9	–	531.8	–	199.1 200.9	Elimination of $HCl/H_2O/Cl_2$	T > 164	Iron oxides/ oxyhydroxides
$Fe(OH)_3$/ferrihydrite	710.9	–	531.8	–	–	Dehydroxylation	200–458.6	Iron oxides
FeO(OH	710.9	530.1	531.8	–	–	Dehydroxylation	200–458.6	Iron oxides
C-steel/1.0/mol/L HCl solution containing 10/mmol/L APSA								
FeO(OH) anhydrous and hydrated	710.8	530.3	531.9	533.3	–	Desorption of physically adsorbed water	50–167.2	Stable corr. product
$Fe^{3+}O(OH, Cl)$	710.8	–	531.9	533.3	199.2 200.9	Elimination of $HCl/H_2O/Cl_2$	T > 167	Iron oxides/ oxyhydroxides
$Fe(OH)_3$/ferrihydrite	710.8	–	531.9	–	–	Dehydroxylation	200–443.8	Iron oxides
FeO(OH)	710.8	530.3	531.9	–	–	Dehydroxylation	200–443.8	Iron oxides

Results of thermal analysis in the present case are slightly different from the earlier reported ones, presumably because of the method of obtaining the Fe^{3+} compounds adopted in this study [28–32]. The use of different precursors affects the thermal curves of the thermal decomposition [30]. When the precursors of the iron oxyhydroxides are sulfate or chloride, the beginning of hematite formation occurs at higher temperatures [30]. Moreover, composition and microstructure will influence the kinetics of the dehydroxylation of goethite [33].

Figure 5a shows TG/DTG/DSC/DTA curves for corrosion products formed on carbon steel surface in 1.0 mol L^{-1} HCl solution in the absence of APSA. Five different mass loss steps were found: (1) up to 131.5 °C (m. loss—11.4%); (2) between 131.5 and 164.5 °C (m. loss—10.7%); (3) between 164.5 and 292 °C (m. loss—3%); (4) between 292 and 400.8 °C (m. loss—22.4%); and (5) between 400.8 and 458.6 °C (m. loss—20.6%). Steps 1 and 2, on TG curve, were evidently due to the hygroscopic moisture. The process is associated with adsorbed non-structural moisture being driven out of the corrosion product particles ($\sim$22.1%). The peaks observed in the region 50–164.4 °C, on the DTG curve at 131.5 and 164.5 °C, can be ascribed to the water desorption and dehydration of the corrosion product [34]. These were accompanied by two endothermic peaks on DSC and DTA curves, at 131.5 and 164.5 °C. Step 3 (on TG curve) can clearly be separated, indicating the presence of various types of impurities, such as Cl ions inserted in FeO(OH) structure. Also, the mass loss of 3% (on TG curve), more probable, reveals the release of different types of the gases, like hydrochloric acid, Cl_2, and/or water from FeO(OH) [33–38]. Steps 4 and 5 were continuous and could not clearly be separated, indicating the presence of hydroxyls from FeO(OH). These appear to be reflected in the complexity of FeO(OH) structure. The mass loss due to dehydroxylation (on TG curves) starts at $t > 200$ °C and finishes at 458.6 °C. In this region of DTG curve, the peak centered at 400.8 °C corresponds to the dehydroxylation of iron oxyhydroxides [32]. Hydroxyl groups in the oxyhydroxide structure are lost as water. Additional endothermic shoulder centered at 317.1 °C is observed on DSC and DTA curves. It indicates the phase transition from goethite [α-FeO(OH)] to hematite [33] and lepidocrocite [γ-FeO(OH)] to maghemite [35]. The irreversible transformation of goethite to hematite occurs, as expected, over a temperature range centered around 300 °C [33]. Therefore, steps 4 and 5 were due to the dehydroxylation of FeO(OH), FeO(OH)·H_2O [36–38], and ferrihydrite [28] at iron oxides [32–38]. Total mass loss was 68.1%.

Figure 5b shows TG/DTG/DSC/DTA curves for the rust formed by the corrosion of carbon steel in 1.0 mol L^{-1} HCl solution in the presence of APSA. The analyses show the following steps:

(i) 50–167.2 °C: corrosion products are stable; mass loss of 21.1% is ascribed to desorption of water (peaks at 130.3 and 167.2 °C on DTG curve and endothermic peaks on DSC and DTA curves at 130.3 and 167.2 °C); (ii) 167.2–287.4 °C: one-step mass loss of 3.9%—release of hydrochloric acid/Cl_2 and/or water; (iii) 287.4–443.8 °C: step mass loss of 41.2%—dehydroxylation of FeO(OH), FeO(OH)·H_2O [36–38], and ferrihydrite [28]; on DTA curve: endothermic effect (shoulder centered at 286 °C) and a peak at 402.8 °C. These steps reveal the same product of corrosion process. The small endothermic peak observed at 402.8 °C in DSC and DTA may be due to the elimination of water from FeO(OH) and/or elimination of gases such as sulfur dioxide and carbon dioxide which could be, more or less the hypothetical result, of APSA decomposition. Total mass loss was 66.2%. The red iron oxide, after corrosion product decomposition, was observed. The results of XPS analysis and TG results are presented in Table 1.

Conclusions

APSA is a good inhibitor for corrosion of carbon steel in 1.0 mol L^{-1} HCl solution.

Mass loss measurements showed that corrosion rate of carbon steel is retarded by APSA and that the inhibition efficiency of inhibitor increases with increasing the concentration, reaching a maximum value of 85.4% at 10 mmol L^{-1} APSA in 1.0 mol L^{-1} HCl solution.

XPS analysis demonstrated that, at this stage, the main product of corrosion is a non-stoichiometric Fe^{3+} oxyhydroxide, consisting of a mixture of FeO(OH) and [FeO(OH)·nH_2O], containing Cl^- ions and adsorbed APSA molecules.

The adsorption mechanism was explained on the basis of the chemical structure and adsorption active centers of the sulfacetamide. Relationship between molecular structure and their inhibition efficiency was elucidated by quantum chemical calculations using the DFT.

The corrosion products were analyzed using TG/DSC/DTA technique. This analysis mainly indicated desorption of physically adsorbed water, elimination of other gases such as hydrochloric acid and Cl_2, and the dehydroxylation of corrosion products at iron oxides.

Acknowledgements This study was supported by CNCSIS-UEFISCSU, project number PNII-IDEI 422/2008.

References

1. Larabi L, Harek Y, Traisnel M, Mansri A. Synergetic influence of poly(4-vinylpyridine) and potassium iodide on inhibition of corrosion of mild steel in 1 M HCl. J Appl Electrochem. 2004;34:833–9.
2. Samide A, Bibicu I, Rogalski M, Preda M. Study of the corrosion inhibition of carbon-steel in dilute ammoniacal media using

N-cyclohexyl-benzothiazole-sulfenamide. Corros Sci. 2005;47:1119–27.
3. Subramania A, Kalyana Sundaram NT, Sathiya Priya R, Saminathan K, Muralidharan VS, Vasuedevan T. Aldimines—effective corrosion inhibitors for mild steel in hydrochloric acid solution. J Appl Electrochem. 2004;34:1–4.
4. Samide A, Bibicu I. Kinetics corrosion process of mild steel in hydrochloric acid in absence and presence of 2-(cyclohexylaminomercapto) benzothiazole. Surf Interface Anal. 2008;40:944–52.
5. Abd El-Rehim SS, Refay SAM, Taha F, Saleh MB, Ahmed RA. Corrosion inhibition of mild steel in acidic medium using 2-amino thiophenol and 2-cyanomethyl benzothiazole. J Appl Electrochem. 2001;31:429–35.
6. Samide A, Bibicu I, Agiu M, Preda M. Mössbabauer spectroscopy study on the corrosion inhibition of mild steel in hydrochloric acid solution. Mater Lett. 2008;62:320–2.
7. Hassan N, Holze R. A comparative electrochemical study of electrosorbed 2- and 4-mercaptopyridines and their application as corrosion inhibitors at C60 steel. J Chem Sci. 2009;121:693–701.
8. Samide A, Bibicu I, Rogalski MS, Preda M. A study of the corrosion inhibition of carbon steel in diluted ammonia media using 2-mercapto benzothiazole by Mössbauer spectrometry. Acta Chim Slov. 2004;51:127–36.
9. Samide A, Bibicu I, Turcanu E. Surface analysis of inhibitor films formed by *N*-(2-hydroxybenzylidene) thiosemicarbazide on carbon steel in acidic media. Chem Eng Commun. 2009;196:1008–17.
10. Samide A, Tutunaru B, Negrila C, Trandafir I, Maxut A. Effect of sulfacetamide on the composition of corrosion products formed onto carbon steel surface in hydrochloric acid. Dig J Nanomater Bios. 2011;6:663–73.
11. Ahamad I, Prasad R, Quraishi MA. Inhibition of mild steel corrosion in acid solution by pheniramine drug: experimental and theoretical study. Corros Sci. 2010;52:198–204.
12. Fonda AS, Mostafa HA, El-Abbasy HM. Antibacterial drugs as inhibitors for the corrosion of stainless steel type 304 in HCl solution. J Appl Electrochem. 2010;40:163–73.
13. Obot IB, Obi-Egbedi NO. 2,3-Diphenylbenzoquinoxaline: a new corrosion inhibitor for mild steel in sulphuric acid. Corros Sci. 2010;52:282–5.
14. Shukla SK, Singh AK, Ahamad I, Quraishi MA. Streptomycin: a commercially available drug as corrosion inhibitor for carbon steel in hydrochloric acid solution. Mater Lett. 2009;63:819–22.
15. El-Naggar MM. Corrosion inhibition of mild steel in acidic medium by some sulfa drugs compounds. Corros Sci. 2007;49:2226–36.
16. Abdallah M. Antibacterial drugs as corrosion inhibitors for corrosion of aluminium in hydrochloric solution. Corros Sci. 2004;46:1981–96.
17. Ebenso EE, Arslan T, Kandemirli F, Love I, Ödretır C, Saracoğlu M, Umoren SA. Theoretical studies of some sulphonamides as corrosion inhibitors for mild steel in acidic medium. Int J Quantum Chem. 2010;110:2614–36.
18. Grosvenor AP, Kobe BA, Biesinger MC, McIntyre NS. Investigation of multiplet splitting of Fe 2p XPS spectra and bonding in iron compounds. Surf Interface Anal. 2004;36:1564–74.
19. Dupin JC, Gonbeau D, Vinatier P, Levasseur A. Systematic XPS studies of metal oxides, hydroxides and peroxides. Phys Chem Chem Phys. 2000;2:1319–24.
20. Yi ZA, Xu YY, Zhu LP, Dong HB, Zhu BK. Hydrophilic modification of peak porous membranes via aqueous surface-initiated atom transfer radical polymerization. Chin J Polym Sci. 2009;27:695–702.
21. Vinnichenko M, Chevolleau T, Pham MT, Poperenko L, Maitz MF. Spectroellipsometric, AFM and XPS probing of stainless steel surfaces subjected to biological influences. Appl Surf Sci. 2002;201:41–50.
22. Billon G, Ouddane B, Gengembre L, Boughriet A. On the chemical properties of sedimentary sulfur in estuarine environments. Phys Chem Chem Phys. 2002;4:751–6.
23. Ait Chikh Z, Chebabe D, Dermaj A, Hajjaji N, Srhiri A, Montemor MF, Ferreira MGS, Bastos AC. Electrochemical and analytical study of corrosion inhibition on carbon steel in HCl medium by 1,12-bis(1,2,4-triazolyl)dodecane. Corros Sci. 2005;47:447–59.
24. Gece G. The use of quantum chemical methods in corrosion inhibitor studies. Corros Sci. 2008;50:2981–92.
25. El Ashry ESH, El Nemr A, Essawy SA, Ragab S. Corrosion inhibitors part 3: quantum chemical studies on the efficiencies of some aromatic hydrazides and Schiff bases as corrosion inhibitors of steel in acidic medium. Arkivoc. 2006;11:205–20.
26. Behpour M, Ghoreishi SM, Soltani N, Salavati-Niasari M, Hamadanian M, Gandomi A. Electrochemical and theoretical investigation on the corrosion inhibition of mild steel by thiosalicylaldehyde derivatives in hydrochloric acid solution. Corros Sci. 2008;50:2172–81.
27. Obot IB, Obi-Egbedi NO, Umoren SA. The synergistic inhibitive effect and some quantum chemical parameters of 2,3-diaminonaphthalene and iodide ions on the hydrochloric acid corrosion of aluminium. Corros Sci. 2009;51:276–82.
28. Jae-Yung Yu, Park M, Kim J. Solubilities of synthetic schwertmannite and ferrihydrite. Geochem J. 2002;36:119–32.
29. Prasad SVS, Sitakara Rao V. Thermal transformation of iron (111) oxide hydrate gel. J Mater Sci. 1984;19:3266–70.
30. Oliviera C, Marchetti GS, Do Carmo Rangel M. The effect the starting material on the thermal decomposition of iron oxyhydroxides. J Therm Anal Calorim. 2003;73:233–40.
31. Barron V, Torrent J, De Grave E. Hydromaghemite, an intermediate in the hydrothermal transformation of 2-line ferrihydrite into hematite. Am Mineral. 2003;88:1679–88.
32. Shah Singh S, Kodama H. Effect of the presence of aluminum ions in iron solutions on the formation of iron oxyhydroxides (FeOOH) at room temperature under acidic environment. Clay Clay Miner. 1994;42:606–13.
33. Gialanella S, Girardi F, Ischia G, Lonardelli I, Mattarelli M, Montagna M. On the goethite to hematite phase transformation. J Therm Anal Calorim. 2010;102:867–73.
34. Rivas Mercury JM, Cabral AA. Thermal behavior and evolution of the mineral phases of Brazilian red mud. J Therm Anal Calorim. 2011;104:635–43.
35. Dinesen AR, Pedersen CT, Bender Koch C. The thermal conversion of lepidocrocite (γ-FeOOH) revisited. J Therm Anal Calorim. 2001;64:1303–10.
36. Przepiera K, Przepiera A. Thermal transformations of selected transition metals oxyhydroxides. J Therm Anal Calorim. 2003;74:659–66.
37. Walter D, Buxbaum G. The mechanism of the thermal transformation from goethite to hematite. J Therm Anal Calorim. 2001;63:733–48.
38. Przepiera K, Przepiera A. Kinetics of thermal transformations of precipitated magnetite and goethite. J Therm Anal Calorim. 2001;65:497–503.